

Strong localization of light in a closely packed granular medium

V. V. Maksimenko, V. A. Krikunov, and A. A. Lushnikov

L. Ya. Karpov Scientific-Research Physicotechnical Institute of the Russian Academy of Sciences

(Submitted 14 April 1992)

Zh. Eksp. Teor. Fiz. 102, 1571–1586 (November 1992)

We study the transformation of a photon, propagating in a close-packed system of strong scatterers (small metallic particles) at frequencies close to the frequency of the dipole surface plasmon in an isolated particle, into a standing electromagnetic wave localized in a bounded region of space with characteristic size of the order of the wavelength λ of the photon ($\lambda \gg R \approx \delta$, R is the particle size, and δ is the distance between particles). It is shown that the localization is due to the distortion produced in the characteristic Rayleigh scattering phase function of an isolated scatterer by cooperative interference effects occurring in a system of random close-packed scatterers. The scattering phase function which is initially symmetric in the forward and backward directions, “swells” into the back hemisphere. Strong localization results in effective absorption of light even if the system consists of absolutely nonabsorbing particles.

1. INTRODUCTION

The phenomenon of localization of electromagnetic waves propagating in a disordered medium is now an independent field of research.¹ As is well known, weak and strong localization are distinguished. Weak localization refers to interference effects accompanying scattering of waves strictly backwards. The trajectory of a photon in this case is an infinitely narrow loop and it is impossible to distinguish the direction in which the photon goes around the loop. The gist of the weak-localization phenomenon, studied, for example, in Refs. 2–7, is constructive interference of the probability amplitudes corresponding to the two alternative possibilities of going around the loop (clockwise and counterclockwise) and resulting in an anomalous increase in the backscattered signal.

The phenomenon of strong localization usually arises when long-wavelength radiation propagates in a disordered system of close-packed scatterers which are small in the sense that the radiation wavelength $\lambda \gg R \approx \delta$, where R is the characteristic size of the scatterers and δ is the average distance between the scatterers. Since the photon wavelength encompasses an entire group of particles, it is impossible in principle to obtain information about the trajectory of a photon in the system. For this reason, in order to calculate the probability W of any electrodynamic process we must first sum the probability amplitudes A_i of all possible ways by which the process can be realized and then calculate the total probability as the squared modulus of the total amplitude $W = |\sum_i A_i|^2$ and not as the sum of the partial probabilities ($W = \sum_i |A_i|^2$), as is done in the classical calculation. In so doing, so-called cross or interference terms $A_i A_j^*$ ($i \neq j$) appear in the expression for the probability of the process. It may seem at first glance that because the particles are distributed randomly in a region of characteristic size $\sim \lambda$ the phases of all partial amplitudes will be random and there will be no interference. This is not the case, however, and there exist at least two types of processes the interference of whose probability amplitudes is in no way affected by the randomness. First, a photon can pass in the forward and backward directions along the same open chain of particles lying in a region of characteristic size $\sim \lambda$. The phases corresponding

to these two probability amplitudes are identical and the amplitudes add up. Second, suppose that the photon has a looped trajectory. The photon can follow the loops in two different ways—clockwise and counterclockwise—which in our case are absolutely indistinguishable. The corresponding probability amplitudes behave in the same manner, since the increment to the phase of the photon around the loop is zero. The constructive interference of the probability amplitudes corresponding to the two alternative ways of going around a loop gives rise to anomalously strong scattering of light into the back hemisphere. This, in turn, stimulates the production of new loops on the trajectory of the photon, and so on. A kind of feedback mechanism is established, and as a result the photon becomes stuck in the system of loops and is trapped in a bounded spatial region of characteristic size $\sim \lambda$.

This is the gist of the phenomenon of strong or Anderson localization of light (see also Refs. 8 and 9).

Thus weak and strong localization are both caused by the interference of virtual photons going around a loop in the photon trajectory. In the first case, however, the entire trajectory is a degenerate (infinitely narrow) loop, whereas in the second case the loops develop on arbitrary photon trajectories.

Strong localization of light is a quite capricious phenomenon and by no means observable in any arbitrary system of scatterers. First of all, the photon elastic scattering length l_s must be less than the photon absorption length l_a . Recall that $l_s = (n_0 \sigma_s)^{-1}$, where σ_s is the elastic light scattering cross section of an individual scatterer and n_0 is the number density of scatterers in the system, and $l_a = (n_0 \sigma_a)^{-1}$, where σ_a is the corresponding absorption cross section. In addition, the elastic light scattering length l_s must be of the order of the photon wavelength λ (in the case $l_s \gg \lambda$ there is no localization, and the situation $l_s < \lambda$ is meaningless).

It may appear at first glance that because of the smallness of the elastic light-scattering cross section of an individual scatterer ($\sigma_s / \pi R^2 \approx (R/\lambda)^4 \ll 1$) the parameter $\rho = \lambda/l_s$, which determines the probability of strong localization, remains negligibly small, even with the maximum

possible packing factor. This is indeed the case, but the situation changes if the frequency of the incident photon is equal to the frequency of a characteristic electromagnetic mode of an individual scatterer. An example of such a mode is a surface plasmon, if the individual particle is metallic. Thus, for example, at frequencies close to the frequency ω_1 of a dipole surface plasmon in a spherical metallic granule ($\omega_1 = 3^{-1/2}\omega_0$, where ω_0 is the classical plasma frequency of the electron gas of the metal) the cross section for elastic light scattering by the particle

$$\sigma_s = \frac{8}{3} \pi R^2 \left(\frac{2\pi R}{\lambda} \right)^4 \frac{\omega^4}{(\omega^2 - \omega_1^2)^2 + g^2 \omega_1^4}$$

has a sharp peak, since for many metals the plasma-resonance width g is usually $\sim 10^{-2}$ (Ref. 10). In this case the parameter $p \approx (R/\lambda)^3 f/g^2$ reaches unity for particles with $R/\lambda \sim 10^{-1}$ already for $f \approx 10^{-1}$ ($f = \frac{4}{3} \pi R^3 n_0$ is the particle packing factor of the system). The photon absorption length l_a ($\sigma_a = 8\pi^2 R^3 g \omega^4 / \lambda [(\omega^2 - \omega_1^2)^2 + g^2 \omega_1^4]$) remains comparable to l_s , i.e., at external radiation frequencies of order ω_1 (the optical-UV range of the spectrum) a close-packed system of small metallic particles is a suitable candidate for observing the localization phenomenon. Metallic particles with such parameters are widely employed in modern technologies and their anomalous optical properties are the subject of lively discussions.¹⁰

Our problem will be to calculate the elastic light-scattering and light-absorption cross sections of close-packed particles, taking into account strong photon localization. We shall show that a photon entering the system will become trapped in a region of characteristic size $\sim \lambda \approx l_s$. We shall find that the physical reason for localization is anomalous scattering of light into the back hemisphere by an individual scatterer of the system owing to cooperative effects. Photon trapping in the system will be formally expressed in the fact that the plasmon-polariton mode acquires the character of a standing wave. We shall verify this by investigating the law of dispersion of a plasmon-polariton. The transformation of the external radiation into standing waves results in anomalously high attenuation of the incident light by close-packed particles. The physical reason for the attenuation is accumulation of energy in the system.

2. DIAGRAMMATIC REPRESENTATION FOR THE AVERAGE ELASTIC LIGHT-SCATTERING CROSS SECTION. BASIC EQUATIONS

In this section we introduce the diagram technique employed in the problem, with the construction of the perturbation series for the differential elastic scattering cross section as the example.

Consider the propagation of a photon with wavelength λ in a system consisting of a large number of spherical metallic particles of radius $R \ll \lambda$. We assume that the average distance between the particles is $\sim R$. The photon elastic scattering amplitude \mathcal{T} , connected with the differential cross section of the process $d\sigma/dn_f$ (n_f is a unit vector in the direction of the scattered photon) by the relation

$$d\sigma/dn_f = |\mathcal{T}|^2$$

is the sum of the following series:

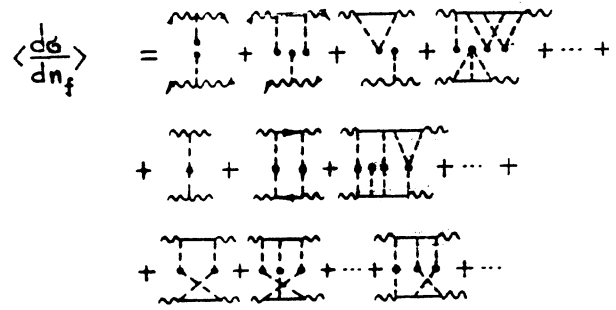


FIG. 1. Perturbation-theory series for the average differential photon elastic scattering cross section of a system of particles.

$$\begin{aligned} \mathcal{T} = & e_{ia} \int \exp(-ik_i \cdot r) \sum_a P_{ab}^a(r, r') e_{fb} \exp(ik_f \cdot r') dr dr' \\ & + e_{ia} \int \exp(-ik_i \cdot r) \sum_a P_{ab}^a(r, r_1) D_{bf}^0(r_1, r_2) \sum_b P_{cv}^b(r_2, r') e_{fv} \\ & \times \exp(ik_f \cdot r') dr dr' dr_1 dr_2 + \dots, \end{aligned} \quad (1)$$

where k is the wave vector of the photon; e is the unit polarization vector; the indices i and f refer to the incident and scattered photons; D^0 is the free-photon propagator in a gauge with zero scalar potential; P^a is the interaction potential between the photon and a particle centered at a point with radius vector a ; and repeated indices are summed over.

Neglecting spatial correlations and averaging the expression (1) over the positions of the particles in the system, it is easy to derive a perturbation series for the averaged elastic-scattering cross section $\langle d\sigma/dn_f \rangle$. Some characteristic terms of this series are presented in diagrammatic form in Fig. 1. Here the wavy lines correspond to the wave functions of the photons $e_{\kappa} e^{\pm ik \cdot r}$; the horizontal lines correspond to single-photon vacuum propagators; the dashed lines correspond to the interaction potential; and, a factor $n_0/(1-f)$ is associated with each dot. The connected diagrams in Fig. 1 correspond to two types of interference processes which occur in the system: 1) ladder diagrams describe the interference of the amplitudes corresponding to the two ways a photon can follow an arbitrary chain of particles belonging to a

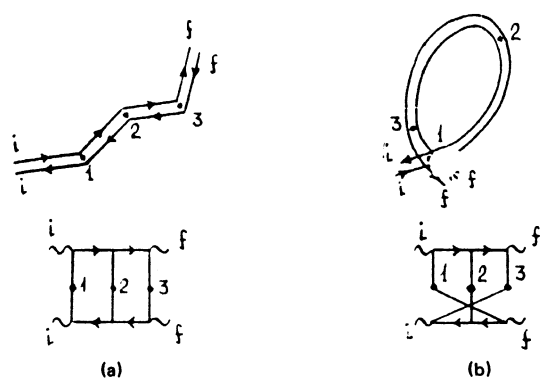


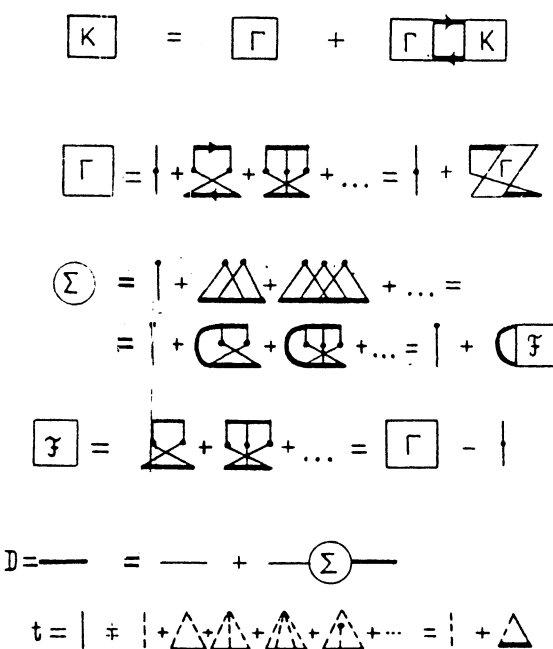
FIG. 2. a) Characteristic ladder diagram describing two interfering processes—forward and backward passage of a chain of particles in a region of characteristic size $\sim \lambda$ by a photon. b) Characteristic fan diagram describing two interfering processes—a photon going clockwise and counterclockwise around a loop in its trajectory.

region of characteristic size $\sim \lambda$ (see Fig. 2a), and 2) fan-shaped diagrams describe the interference of amplitudes corresponding to the two alternative ways a photon can go around a loop along a self-intersecting trajectory (see Fig. 2b). The unconnected diagrams (Fig. 1), which describe coherent scattering of light in the forward direction, do not contribute anything because of the random arrangement of the particles. As one can easily see, the summation of the connected diagrams reduces to the solution, for the two-photon propagator, of the Bethe-Salpeter equation, whose kernel is the sum of the fan diagrams.

The two-photon propagator K is defined in Fig. 3. Here we present equations for the interaction amplitude Γ , the photon mass operator Σ , the single-photon propagator D , and the t -matrix for the scattering of a photon by an isolated particle. The idea of the solution of the system of equations in Fig. 3 consists of trying to guess the correct form of the single-photon propagator D by introducing an unknown parameter and then determining this parameter from the condition that the system be self-consistent. The effective dielectric constant of the system of particles, which appears in the problem in an entirely natural manner, since $R \ll \lambda$, plays the role of the unknown parameter. Thus the main problem reduces to determining the dielectric constant from the condition of self-consistency. The equation for K can be solved then, using the explicit form of Γ and D .

The two-photon propagator K , in accordance with Fig. 3, satisfies the equation

$$K_{\alpha\delta\sigma\nu}(\mathbf{r}_1, \mathbf{r}', \bar{\mathbf{r}}, \bar{\mathbf{r}'}) = \Gamma_{\alpha\delta\sigma\nu}(\mathbf{r}, \mathbf{r}', \bar{\mathbf{r}}, \bar{\mathbf{r}'}) + \int \Gamma_{\alpha\beta\mu\nu}(\mathbf{r}, \mathbf{r}_1, \mathbf{r}_2, \bar{\mathbf{r}'}) D_{\beta\mu}(\mathbf{r}_1, \mathbf{r}_2) \times K_{\nu\sigma\gamma}(\mathbf{r}_2, \mathbf{r}', \bar{\mathbf{r}}, \mathbf{r}_3) D_{\gamma\mu}(\mathbf{r}_3, \mathbf{r}_4) d\mathbf{r}_1 d\mathbf{r}_2 d\mathbf{r}_3 d\mathbf{r}_4. \quad (2)$$



and the interaction amplitude Γ satisfies the equation

$$\begin{aligned} \Gamma_{\alpha\delta\sigma\nu}(\mathbf{r}, \mathbf{r}', \bar{\mathbf{r}}, \bar{\mathbf{r}'}) &= \frac{n_0}{1-f} \int t_{\alpha\delta}(\mathbf{r}, \mathbf{r}') t_{\sigma\nu}(\bar{\mathbf{r}}, \bar{\mathbf{r}'}) d\mathbf{a} \\ &+ \frac{n_0}{1-f} \int t_{\alpha\gamma}(\mathbf{r}, \mathbf{r}_1) \\ &\times D_{\gamma\epsilon}(\mathbf{r}_1, \mathbf{r}_2) \Gamma_{\epsilon\delta\beta\nu}(\mathbf{r}_2, \mathbf{r}', \bar{\mathbf{r}}, \bar{\mathbf{r}'}) D_{\beta\mu}(\mathbf{r}_1, \mathbf{r}_3) t_{\sigma\mu}(\bar{\mathbf{r}}, \mathbf{r}_4) d\mathbf{r}_1 d\mathbf{r}_2 d\mathbf{r}_3 d\mathbf{r}_4. \end{aligned} \quad (3)$$

The photon propagator D satisfies Dyson's equation:

$$\begin{aligned} D_{\alpha\beta}(\mathbf{r}, \mathbf{r}') &= D_{\alpha\beta}^0(\mathbf{r}, \mathbf{r}') \\ &+ \int D_{\alpha\gamma}^0(\mathbf{r}, \mathbf{r}_1) \Sigma_{\gamma\gamma}(\mathbf{r}_1, \mathbf{r}_2) D_{\gamma\beta}(\mathbf{r}_2, \mathbf{r}') d\mathbf{r}_1 d\mathbf{r}_2, \end{aligned} \quad (4)$$

where

$$D_{\alpha\beta}^0(\mathbf{r}, \mathbf{r}') = \left(\delta_{\alpha\beta} - \frac{c^2}{\omega^2} \nabla_\alpha \nabla_\beta \right) \frac{\exp(-i\omega|\mathbf{r}-\mathbf{r}'|c)}{|\mathbf{r}-\mathbf{r}'|}$$

is the free-photon propagator in a gauge with zero scalar potential, Σ is the photon mass operator defined by the expression

$$\begin{aligned} \Sigma_{\alpha\beta}(\bar{\mathbf{r}}, \bar{\mathbf{r}'}) &= \Sigma_{\alpha\beta}(\bar{\mathbf{r}}-\bar{\mathbf{r}'}) = \frac{n_0}{1-f} \int t_{\alpha\beta}(\bar{\mathbf{r}}, \bar{\mathbf{r}'}) d\mathbf{a} \\ &+ \int \mathcal{F}_{\alpha\delta\sigma\nu}(\mathbf{r}, \mathbf{r}', \bar{\mathbf{r}}, \bar{\mathbf{r}'}) D_{\nu\beta}(\bar{\mathbf{r}}, \bar{\mathbf{r}'}) d\bar{\mathbf{r}'} d\mathbf{r}. \end{aligned} \quad (5)$$

and the relationship between the block \mathcal{F} and Γ is given in Fig. 3. The equation for the t -matrix for scattering of a photon by an isolated particle has the form

$$t_{\alpha\beta}(\mathbf{r}, \mathbf{r}') = P_{\alpha\beta}(\mathbf{r}, \mathbf{r}') + \int P_{\alpha\gamma}(\mathbf{r}, \mathbf{r}_1) D_{\gamma\gamma}(\mathbf{r}_1, \mathbf{r}_2) t_{\gamma\beta}(\mathbf{r}_2, \mathbf{r}') d\mathbf{r}_1 d\mathbf{r}_2. \quad (6)$$

Thus we assume that the photon propagator D in the system looks just like the propagator in a uniform effective medium characterized by longitudinal $\bar{\epsilon}_l$ and transverse $\bar{\epsilon}_t$ dielectric constants:

$$\begin{aligned} D_{\alpha\beta}(\mathbf{k}, \omega) &= \int D_{\alpha\beta}(\mathbf{r}, \mathbf{r}') \exp[i\mathbf{k}(\mathbf{r}-\mathbf{r}')] d(\mathbf{r}-\mathbf{r}') \\ &= \frac{4\pi}{(kc)^2 - \omega^2 \bar{\epsilon}_l} \left\{ \delta_{\alpha\beta} - \frac{(kc)^2 - \omega^2 (\bar{\epsilon}_l - \bar{\epsilon}_t)}{\omega^2 \bar{\epsilon}_l} \frac{k_a k_b}{k^2} \right\}. \end{aligned} \quad (7)$$

Substituting the expression (7) for D into Eqs. (2)–(6) we obtain, from the condition of self-consistency, equations for $\bar{\epsilon}_l$ and $\bar{\epsilon}_t$.

3. SOLUTION OF THE EQUATIONS

We start with Eq. (6) for the t -matrix. First we rewrite it in the form

$$\begin{aligned} t_{\alpha\beta}(\mathbf{x}, \mathbf{x}') &= P_{\alpha\beta}(\mathbf{x}, \mathbf{x}') \\ &+ \int P_{\alpha\gamma}(\mathbf{x}, \mathbf{x}_1) D_{\gamma\gamma}(\mathbf{x}_1, \mathbf{x}_2) t_{\gamma\beta}(\mathbf{x}_2, \mathbf{x}') d\mathbf{x}_1 d\mathbf{x}_2, \end{aligned} \quad (8)$$

where $\mathbf{x} = \mathbf{r} - \mathbf{a}$, $\mathbf{x}' = \mathbf{r}' - \mathbf{a}$, and

$$P_{\alpha\beta}(\mathbf{r}, \mathbf{r}') = \frac{\epsilon \delta_{\alpha\beta} \delta(\mathbf{r}-\mathbf{r}') - \epsilon_{\alpha\beta}(\mathbf{r}, \mathbf{r}')}{4\pi} \frac{\omega^2}{c^2} \theta(R-r) \theta(R-r'), \quad (9)$$

FIG. 3. System of basic equations of the problem.

where $\varepsilon(\omega) = 1 - \omega_0^2/\omega^2$ is the dielectric constant of the metal; $\theta(x)$ is the unit step function; and, $\bar{\varepsilon}_{\alpha\beta}(\mathbf{r}, \mathbf{r}')$ is the effective dielectric tensor of the medium

$$\varepsilon_{\alpha\beta}(\mathbf{r}, \mathbf{r}') \equiv \varepsilon_{\alpha\beta}(\mathbf{r}-\mathbf{r}') = (2\pi)^{-3} \int \varepsilon_{\alpha\beta}(\mathbf{k}, \omega) \exp[-i\mathbf{k}(\mathbf{r}-\mathbf{r}')] d\mathbf{k}.$$

and is connected with the longitudinal $\bar{\varepsilon}_l$ and transverse $\bar{\varepsilon}_t$ dielectric constants by the relation¹¹

$$\varepsilon_{\alpha\beta}(\mathbf{k}, \omega) = \varepsilon_t(k, \omega) \left(\delta_{\alpha\beta} - \frac{k_\alpha k_\beta}{k^2} \right) + \bar{\varepsilon}_l(k, \omega) \frac{k_\alpha k_\beta}{k^2}.$$

Using the identity

$$\int \nabla_\alpha \nabla_\beta Q(\mathbf{r}) e^{i\mathbf{k}\mathbf{r}} d\mathbf{r} = -4\pi k_\alpha k_\beta / k^2,$$

where $Q(\mathbf{r}) = |\mathbf{r}|^{-1}$, it is easy to establish the explicit form of $\bar{\varepsilon}_{\alpha\beta}(\mathbf{r}, \mathbf{r}')$, which we shall employ below:

$$\begin{aligned} \varepsilon_{\alpha\beta}(\mathbf{r}, \mathbf{r}') &= \varepsilon_t \left[\delta_{\alpha\beta} \delta(\mathbf{r}-\mathbf{r}') - \frac{1}{4\pi} \nabla_\alpha \nabla_\beta' Q(\mathbf{r}, \mathbf{r}') \right] \\ &\quad + \frac{1}{4\pi} \bar{\varepsilon}_l \nabla_\alpha \nabla_\beta' Q(\mathbf{r}, \mathbf{r}). \end{aligned} \quad (10)$$

We require the t -matrix inside a particle. For this reason, for $R \ll \lambda$ we can drop in the propagator D in Eq. (8) the terms containing the small parameter $\omega R/c$ characterizing the retardation of the electromagnetic interaction, and we represent D in the form

$$D_{\alpha\beta}(\mathbf{r}, \mathbf{r}') = -\frac{c^2}{\varepsilon_t \omega^2} \nabla_\alpha \nabla_\beta' Q(\mathbf{r}, \mathbf{r}'). \quad (11)$$

Now we seek the solution of Eq. (8) in the form

$$t_{\alpha\beta}(\mathbf{r}, \mathbf{r}') = P_{\alpha\beta}(\mathbf{r}, \mathbf{r}') + \theta(R-r) \theta(R-r') \omega^2 \nabla_\alpha \nabla_\beta' F(\mathbf{r}, \mathbf{r}').$$

After substituting the expressions (9), (10), and (11) into Eq. (8) we obtain the following equation for the function F :

$$\begin{aligned} -\varepsilon_t F(\mathbf{r}, \mathbf{r}') &= \left(\frac{\varepsilon - \bar{\varepsilon}_l}{4\pi} \right)^2 Q(\mathbf{r}, \mathbf{r}') \\ &\quad + \frac{\varepsilon - \bar{\varepsilon}_l}{4\pi} \int \theta(R-r_1) \nabla_{1v} Q(\mathbf{r}, \mathbf{r}_1) \nabla_{1v} \\ &\quad \times \left[\frac{2(\varepsilon_t - \bar{\varepsilon}_l)}{(4\pi)^2} Q(\mathbf{r}_1, \mathbf{r}') + F(\mathbf{r}_1, \mathbf{r}') \right] d\mathbf{r}_1 \\ &\quad + \frac{\bar{\varepsilon}_l - \bar{\varepsilon}_t}{(4\pi)^2} \int \theta(R-r_1) \nabla_{1v} Q(\mathbf{r}, \mathbf{r}_1) \nabla_{1v} \nabla_{2v} \\ &\quad \times Q(\mathbf{r}_1, \mathbf{r}_2) \theta(R-r_2) \nabla_{2v} \left[\frac{\bar{\varepsilon}_l - \bar{\varepsilon}_t}{(4\pi)^2} Q(\mathbf{r}_2, \mathbf{r}') + F(\mathbf{r}_2, \mathbf{r}') \right] d\mathbf{r}_1 d\mathbf{r}_2. \end{aligned} \quad (12)$$

We seek the solution of Eq. (12) in the form of an expansion in scalar spherical harmonics. In the dipole approximation we have

$$t_{\alpha\beta}(\mathbf{r}, \mathbf{r}') = A \theta(R-|a-r|) \theta(R-|a-r'|) \omega^2 \delta_{\alpha\beta} \delta(\mathbf{r}-\mathbf{r}'), \quad (13)$$

where

$$A = \frac{3}{4\pi} \bar{\varepsilon}_l \frac{3(\varepsilon - \bar{\varepsilon}_l) - (\bar{\varepsilon}_l - \bar{\varepsilon}_t)}{3(\varepsilon + 2\bar{\varepsilon}_l) + 8(\bar{\varepsilon}_l - \bar{\varepsilon}_t)}. \quad (14)$$

Using the expression (13), we rewrite Eq. (3) in the following form:

$$\begin{aligned} \Gamma_{\alpha\delta\sigma\nu}(\mathbf{r}, \mathbf{r}', \bar{\mathbf{r}}, \bar{\mathbf{r}'}) &= \delta_{\alpha\delta} \delta_{\sigma\nu} \delta(\mathbf{r}-\mathbf{r}') \delta(\bar{\mathbf{r}}-\bar{\mathbf{r}'}) \varphi(\mathbf{r}-\bar{\mathbf{r}}) \\ &\quad + \varphi(\mathbf{r}-\bar{\mathbf{r}}) \int D_{\alpha\epsilon}(\mathbf{r}, \mathbf{r}_1) \Gamma_{\epsilon\delta\sigma\nu}(\mathbf{r}_1, \mathbf{r}', \bar{\mathbf{r}}, \bar{\mathbf{r}'}) D_{\sigma\epsilon}(\bar{\mathbf{r}}, \mathbf{r}_2) d\mathbf{r}_1 d\mathbf{r}_2, \end{aligned}$$

where

$$\begin{aligned} \varphi(\mathbf{r}-\bar{\mathbf{r}}) &= \frac{n_0}{1-f} \omega^4 |A|^2 \int \theta(R-|a-r|) \theta(R-|a-\bar{\mathbf{r}}|) da \\ &= \frac{n_0}{1-f} \omega^4 |A|^2 \cdot \frac{2}{3} \pi t^2 (3R-t) \theta(t) \end{aligned}$$

and $t = R - |\mathbf{r} - \bar{\mathbf{r}}|/2$. The substitution

$$\begin{aligned} \Gamma_{\alpha\delta\sigma\nu}(\mathbf{r}, \mathbf{r}', \bar{\mathbf{r}}, \bar{\mathbf{r}'}) &= \delta_{\alpha\delta} \delta_{\sigma\nu} \delta(\mathbf{r}-\mathbf{r}') \delta(\bar{\mathbf{r}}-\bar{\mathbf{r}'}) \varphi(\mathbf{r}-\bar{\mathbf{r}}) \\ &\quad + \frac{\partial^4}{\partial r_\alpha \partial r'_\delta \partial \bar{r}_\sigma \partial \bar{r}'_\nu} \Phi(\mathbf{r}, \mathbf{r}', \bar{\mathbf{r}}, \bar{\mathbf{r}'}) \end{aligned}$$

gives the following equation for the function Φ :

$$\begin{aligned} &\frac{\partial^4}{\partial r_\alpha \partial r'_\delta \partial \bar{r}_\sigma \partial \bar{r}'_\nu} \Phi(\mathbf{r}, \mathbf{r}', \bar{\mathbf{r}}, \bar{\mathbf{r}'}) \\ &= \varphi(\mathbf{r}-\bar{\mathbf{r}}) \varphi(\mathbf{r}'-\bar{\mathbf{r}'}) D_{\alpha\epsilon}(\mathbf{r}, \mathbf{r}') D_{\sigma\epsilon}(\bar{\mathbf{r}}, \bar{\mathbf{r}'}) \\ &\quad + \varphi(\mathbf{r}-\bar{\mathbf{r}}) \frac{\partial^2}{\partial r'_\delta \partial \bar{r}'_\nu} \int D_{\alpha\epsilon}(\mathbf{r}, \mathbf{r}_1) \\ &\quad \times \frac{\partial^2}{\partial r_{1\epsilon} \partial r_{2\delta}} \Phi(\mathbf{r}_1, \mathbf{r}', \bar{\mathbf{r}}, \bar{\mathbf{r}'}) D_{\sigma\epsilon}(\bar{\mathbf{r}}, \mathbf{r}_2) d\mathbf{r}_1 d\mathbf{r}_2. \end{aligned} \quad (15)$$

Since the particles are close-packed, the coordinates of the single-particle propagators in the equations for K , Γ , and Σ are separated by a distance $\sim R$. This makes it possible to neglect retardation effects in these equations and, once again, to represent D in the form (11), as we already did in solving Eq. (8) [as far as Eq. (15) is concerned, this procedure can also be used for rarefied systems, since the propagators D in Eq. (15) describe the propagation of a photon along a loop of a self-intersecting trajectory and their coordinates are always separated by the distance $\sim R$]. Taking this into account, integrating by parts in Eq. (15), and using the identity $\Delta Q(\mathbf{r}) = -4\pi|\mathbf{r}|^{-1}$, we have

$$\Gamma_{\alpha\delta\sigma\nu}(\mathbf{r}, \mathbf{r}', \bar{\mathbf{r}}, \bar{\mathbf{r}'}) = \Gamma_{\alpha\delta\sigma\nu}(\mathbf{r}-\bar{\mathbf{r}}, \mathbf{r}'-\bar{\mathbf{r}'}, \mathbf{r}-\mathbf{r}')$$

$$\begin{aligned} &= \Gamma_{\alpha\delta\sigma\nu}(\mathbf{r}_1, \mathbf{r}_2, \mathbf{r}_3) = \delta_{\alpha\delta} \delta_{\sigma\nu} \delta(\mathbf{r}_3) \\ &\quad \times \delta(\mathbf{r}_1-\mathbf{r}_2) \varphi(\mathbf{r}_1) + \frac{\varphi(\mathbf{r}_2) \varphi(\mathbf{r}_1)}{1-\gamma^2 \varphi(\mathbf{r}_1)} D_{\alpha\delta}(\mathbf{r}_3) D_{\sigma\nu}(\mathbf{r}_3+\mathbf{r}_2-\mathbf{r}_1) \\ &= \delta_{\alpha\delta} \delta_{\sigma\nu} \delta(\mathbf{r}_3) \delta(\mathbf{r}_1-\mathbf{r}_2) \varphi(\mathbf{r}_3) + \mathcal{F}_{\alpha\delta\sigma\nu}(\mathbf{r}_1, \mathbf{r}_2, \mathbf{r}_3), \end{aligned} \quad (16)$$

where $\gamma = 4\pi/|\bar{\varepsilon}_l|\omega^2$. After substituting \mathcal{F} into Eq. (5) and switching to the momentum representation in Eq. (4), we obtain for the Fourier transform of D the expression (7), where $\bar{\varepsilon}_l$ and $\bar{\varepsilon}_t$ satisfy the system of equations

$$\bar{\varepsilon}_t = 1 + 4\pi g A,$$

$$\bar{\varepsilon}_t - \bar{\varepsilon}_l = \frac{g(4\pi A)^4}{\bar{\varepsilon}_l [\bar{\varepsilon}_l^2 - (4\pi A)^2]},$$

where $g = f/(1-f)$ and A is defined by the expression (14).

Thus the problem of determining the effective dielectric constant has been solved and we can proceed to Eq. (2) for

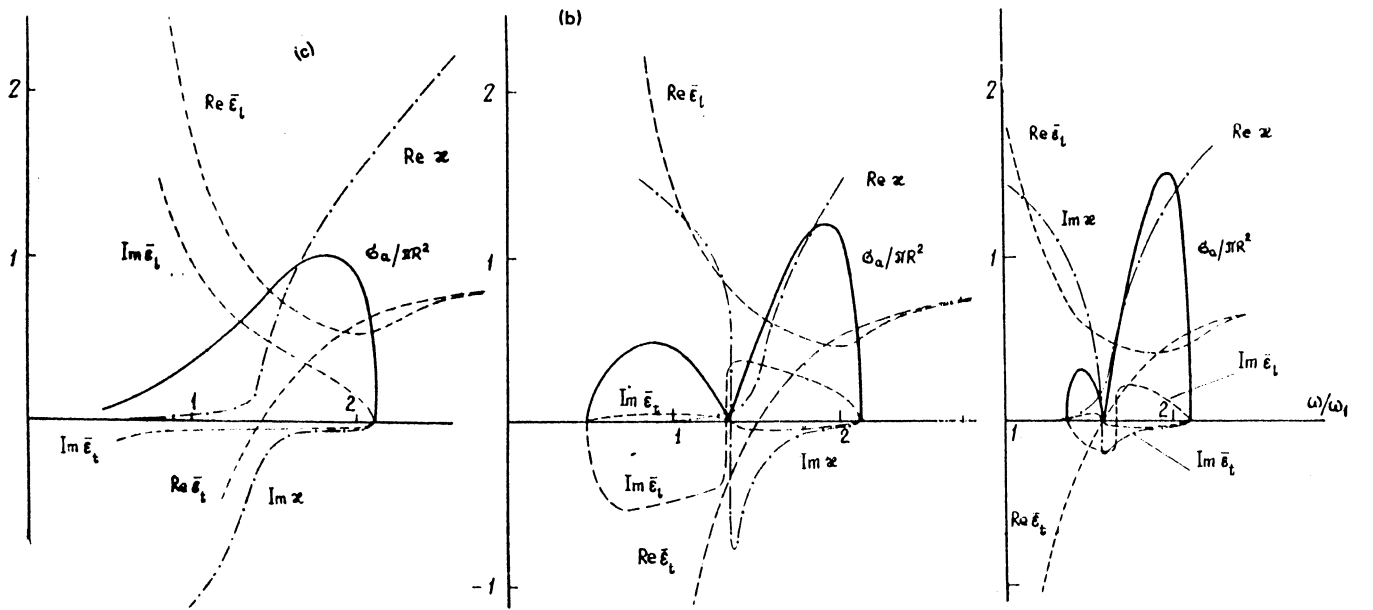


FIG. 4. Frequency dependence of the real and imaginary parts of the effective dielectric constants of the system, the wave vector ($\omega = kc/\omega_1$) of a plasmon-polariton in the system, and the absorption cross section $\sigma_a/\pi R^2$ per particle. The particle radius $R = 300 \text{ \AA}$, $\omega_1 R/c = 0.53$, and the packing factor $f = 0.5$ (a), 0.6 (b), and 0.7 (c).

K. It is convenient to seek the solution of this equation in the form

$$K_{\alpha\delta\sigma}(\mathbf{r}, \mathbf{r}', \bar{\mathbf{r}}, \bar{\mathbf{r}'}) = \Gamma_{\alpha\delta\sigma}(\mathbf{r}, \mathbf{r}', \bar{\mathbf{r}}, \bar{\mathbf{r}'}) + \frac{\partial^4}{\partial r_\alpha \partial r'_\delta \partial \bar{r}_\sigma \partial \bar{r}'_\sigma} L(\mathbf{r}, \mathbf{r}', \bar{\mathbf{r}}, \bar{\mathbf{r}'}). \quad (18)$$

Substituting the expression (18) into Eq. (2) and integrating by parts gives

$$\begin{aligned} & \frac{\partial^4}{\partial r_\alpha \partial r'_\delta \partial \bar{r}_\sigma \partial \bar{r}'_\sigma} L(\mathbf{r}, \mathbf{r}', \bar{\mathbf{r}}, \bar{\mathbf{r}'}) \\ &= \frac{\varphi(\mathbf{r}-\bar{\mathbf{r}'})\varphi(\mathbf{r}'-\bar{\mathbf{r}})D_{\alpha\delta}(\mathbf{r}, \mathbf{r}')D_{\sigma\sigma'}(\bar{\mathbf{r}}, \bar{\mathbf{r}'})}{1-\gamma^2\varphi(\mathbf{r}-\bar{\mathbf{r}'})+\gamma^2\varphi(\mathbf{r}-\bar{\mathbf{r}})/[1-\gamma^2\varphi(\mathbf{r}-\bar{\mathbf{r}'})]}. \end{aligned}$$

It is convenient to represent the final expression for K in the form

$$\begin{aligned} K_{\alpha\delta\sigma\sigma'}(\mathbf{r}, \mathbf{r}', \bar{\mathbf{r}}, \bar{\mathbf{r}'}) &= K_{\alpha\delta\sigma\sigma'}(\mathbf{r}_1, \mathbf{r}_2, \mathbf{r}_3) = \delta_{\alpha\delta}\delta_{\sigma\sigma'}\delta(\mathbf{r}_3)\delta(\mathbf{r}_1-\mathbf{r}_2)\varphi(\mathbf{r}_1) \\ &+ \gamma^2(2\pi)^{-6} \int \frac{k_\alpha k_\delta}{k^2} \frac{s_\sigma s_{\sigma'}}{s^2} \\ &\times \exp(-ik\mathbf{r}_3) \exp(is(\mathbf{r}_2+\mathbf{r}_3-\mathbf{r}_1)) dk ds \left\{ \frac{\varphi(\mathbf{r}_2)\varphi(\mathbf{r}_1)}{1-\gamma^2\varphi(\mathbf{r}_1)} \right. \\ &\left. + \frac{\varphi(\mathbf{r}_2+\mathbf{r}_3)\varphi(\mathbf{r}_1-\mathbf{r}_3)[1-\gamma^2\varphi(\mathbf{r}_2+\mathbf{r}_3)]}{1-2\gamma^2\varphi(\mathbf{r}_2+\mathbf{r}_3)} \right\}. \quad (19) \end{aligned}$$

Figure 4 shows the frequency dependences of the dielectric constants $\bar{\epsilon}_t$ and $\bar{\epsilon}_l$, calculated in accordance with Eqs. (17), for different packing factors. The figure also shows the plasmon-polariton dispersion curve for a system described by the relation $\omega = ck/\sqrt{\bar{\epsilon}_t}$.

It is easy to see that as the frequency decreases, renor-

malization of the photon velocity is replaced by complete stopping of the photon—the group velocity $d\omega/dk$ of the excitation becomes zero. The excitation then becomes ill-determined ($\text{Im } k \approx \text{Re } k$) and, finally, the wave vector becomes imaginary, in spite of the fact that the system under consideration consists of absolutely nonabsorbing particles. The latter fact is not surprising and is reminiscent of the behavior of the wave vector in a solid metal at frequencies below the classical plasma frequency, when the dielectric constant of the metal is negative. The fact that the wave vector of the excitation is imaginary in this case is associated, as is well known, not with the absorption of the wave, but rather with the reflection of the wave and its transformation into surface electromagnetic modes. The analogy observed in our case is apparently not accidental, since the packing density of the particles in the system is sufficiently high for some characteristic effects of a continuous metal to be reproduced.

The appearance of two effective dielectric constants $\bar{\epsilon}_t$ and $\bar{\epsilon}_l$ is easy to understand. It is well known¹¹ that a difference between $\bar{\epsilon}_t$ and $\bar{\epsilon}_l$ arises, even in a uniform and isotropic medium, when the nonuniformity and nonisotropic nature of the system, which are introduced into the problem by the wave vector \mathbf{k} of the incident electromagnetic wave, are taken into account. The difference between $\bar{\epsilon}_t$ and $\bar{\epsilon}_l$ is $\sim kL$, where L is the characteristic scale of the nonuniformity of the system. In the case of the propagation of a photon in a finely dispersed medium, such as ours, $L \sim R$ (R is the radius of a particle), $kR \sim R/\lambda \ll 1$, and the difference $\bar{\epsilon}_t - \bar{\epsilon}_l$ is insignificant. In the region of localization we have $L \sim l_s \approx \lambda$. For this reason, $\bar{\epsilon}_t - \bar{\epsilon}_l \approx 1$ —in accordance with the computation.

4. SCATTERING AND ABSORPTION OF LIGHT

In this section we investigate the effect of localization on elastic scattering and absorption of light by close-packed metallic particles.

We start with elastic scattering. It is obvious that

$$\begin{aligned} \left\langle \frac{d\sigma}{dn_i} \right\rangle &= e_{ia} e_{ib} e_{ic} e_{iv} \int K_{abcv}(\mathbf{r}, \mathbf{r}', \bar{\mathbf{r}}, \bar{\mathbf{r}'}) \\ &\times \exp[-i(\mathbf{k}_i \cdot \mathbf{r} - \mathbf{k}_f \cdot \mathbf{r}' + \bar{\mathbf{k}}_i \cdot \bar{\mathbf{r}} - \bar{\mathbf{k}}_f \cdot \bar{\mathbf{r}'})] \\ &\times d\mathbf{r} d\mathbf{r}' d\bar{\mathbf{r}} d\bar{\mathbf{r}'} = V e_{ia} e_{ib} e_{ic} e_{iv} \int K_{abcv}(\mathbf{r}_1, \mathbf{r}_2, \mathbf{r}_3) \\ &\times \exp[i(\mathbf{k}_i \cdot \mathbf{r}_1 - i(\mathbf{k}_i + \mathbf{k}_f) \cdot \mathbf{r}_3 - i\mathbf{k}_f \cdot \mathbf{r}_2)] d\mathbf{r}_1 d\mathbf{r}_2 d\mathbf{r}_3, \end{aligned} \quad (20)$$

where V is the volume of the system. It is curious that the integrals in Eq. (20) are nonanalytic functions of the direction of scattering. We now verify this by calculating as an example the contribution of the second term on the right-hand side of the expression (19) for K in $\langle d\sigma/dn_f \rangle$. Carrying out the trivial integration over \mathbf{r}_3 , we have

$$(2\pi)^{-3} \int \frac{\varphi(\mathbf{r}_2)\varphi(\mathbf{r}_1)}{1-\gamma^2\varphi(\mathbf{r}_1)} d\mathbf{r}_1 d\mathbf{r}_2 \int \frac{k_a k_b}{k^2} \frac{(\mathbf{k}_i + \mathbf{k}_f + \mathbf{k})_a (\mathbf{k}_i + \mathbf{k}_f + \mathbf{k})_v}{(\mathbf{k}_i + \mathbf{k}_f + \mathbf{k})^2} \times \exp[i\mathbf{k}(\mathbf{r}_2 - \mathbf{r}_1)] dk. \quad (21)$$

An obvious symmetrization puts the integral over the momenta in the expression (21) into the form

$$\begin{aligned} I &= (2\pi)^{-3} \exp[i(\mathbf{r}_1 - \mathbf{r}_2) \cdot \mathbf{m}] \\ &\times \int \frac{(\mathbf{q} - \mathbf{m})_a (\mathbf{q} - \mathbf{m})_b (\mathbf{q} + \mathbf{m})_a (\mathbf{q} + \mathbf{m})_v}{(\mathbf{q} - \mathbf{m})^2 (\mathbf{q} + \mathbf{m})^2} \\ &\times \exp[i\mathbf{q}(\mathbf{r}_1 - \mathbf{r}_2)] d\mathbf{q}, \end{aligned}$$

where $\mathbf{q} = \mathbf{k} + \mathbf{m}$, $\mathbf{m} = \frac{1}{2}(\mathbf{k}_i + \mathbf{k}_f)$. Since $\mathbf{r}_1, \mathbf{r}_2 \sim R$

$$I = \frac{(\mathbf{k}_i + \mathbf{k}_f)_a (\mathbf{k}_i + \mathbf{k}_f)_b (\mathbf{k}_i + \mathbf{k}_f)_v (\mathbf{k}_i + \mathbf{k}_f)_v}{(\mathbf{k}_i + \mathbf{k}_f)^4} \delta(\mathbf{r}_1 - \mathbf{r}_2) + O(k_i R).$$

The last expression is not defined at $\mathbf{k}_i = -\mathbf{k}_f$. This corresponds to strictly backward scattering. In this case, when integrating over the momenta in the expression (21), it is convenient to use the formula

$$\begin{aligned} (2\pi)^{-3} \int \frac{k_a k_b k_c k_v}{k^4} e^{i\mathbf{k}\mathbf{r}} d\mathbf{k} &= \delta(\mathbf{r}) [4(n_\alpha n_\beta \delta_{\alpha v} + n_\alpha n_\alpha \delta_{\beta v} + n_\alpha n_v \delta_{\beta \alpha}) \\ &- 4n_\alpha n_\beta n_\alpha n_v - \delta_{\alpha \beta} \delta_{\alpha v} - \delta_{\alpha \alpha} \delta_{\beta v} - \delta_{\alpha v} \delta_{\beta \alpha}] \\ &- \frac{1}{\pi r^3} \left[\frac{1}{4} (\delta_{\alpha \beta} \delta_{\alpha v} + \delta_{\alpha \alpha} \delta_{\beta v} + \delta_{\alpha v} \delta_{\beta \alpha}) \right. \\ &\left. + \frac{1}{2} / (n_\alpha n_\beta n_\alpha n_v - \frac{1}{2}(n_\alpha n_\beta \delta_{\alpha v} + n_\alpha n_\alpha \delta_{\beta v} + n_\alpha n_v \delta_{\beta \alpha})) \right], \end{aligned}$$

where $\mathbf{n} = \mathbf{r}/R$.

As a result of such calculations the per-particle differential elastic light-scattering cross section is found to be

$$\begin{aligned} \left\langle \frac{d\sigma}{dn_i} \right\rangle &= \left(\frac{\omega R}{c} \right)^4 \frac{R^2}{1-f} \left| \varepsilon_i \frac{3(\varepsilon - \bar{\varepsilon}_i) - (\bar{\varepsilon}_i - \bar{\varepsilon}_i)}{3(\varepsilon + 2\bar{\varepsilon}_i) + 8(\bar{\varepsilon}_i - \bar{\varepsilon}_i)} \right|^2 \left\{ (e_i e_i)^2 \right. \\ &- \left[\frac{(e_i k_i)^2 (e_i k_i)^2}{(k_i + k_f)^4} (1 - \delta_{k_i, -k_f}) + \frac{1+2(e_i e_i)^2}{15} \delta_{k_i, -k_f} \right] \\ &\times \left(1 + \frac{16}{\alpha^3} + \frac{192}{\alpha^6} \int_0^\alpha \frac{x^2 dx}{x^3 - 3\alpha^2 x^2 + 2\alpha^3 - 4} \right) - \frac{3}{2} \frac{1+2(e_i e_i)^2}{15} \\ &\times \left. \left(\frac{1}{6} + \frac{4}{\alpha^3} - \frac{17}{315} \alpha^3 + \frac{8}{\alpha^6} \int_0^\alpha \frac{x^2 dx}{x^3 - 3\alpha^2 x^2 + 2\alpha^3 - 2} \right) \right\}, \end{aligned} \quad (22)$$

where $\alpha^3 = 18g |[3(\varepsilon - \bar{\varepsilon}_i) - (\bar{\varepsilon}_i - \bar{\varepsilon}_i)]/[3(\varepsilon + 2\bar{\varepsilon}_i) + 8(\bar{\varepsilon}_i - \bar{\varepsilon}_i)]|^2$. The first integral in Eq. (22) for $a < 1$, just as the second integral for $a < 2^{-1/3}$, is

$$\begin{aligned} \frac{1}{3} \frac{1}{(s_1^2 + s_2^2 + s_1 s_2)} &\left\{ (s_1 + s_2)^2 \right. \\ &\times \ln \left| 1 - \frac{\alpha}{s_1 + s_2} \right| + \frac{1}{2} (2s_1^2 + 2s_2^2 + s_1 s_2) \\ &\times \ln \left| 1 + \frac{\alpha^2 + \alpha(s_1 + s_2)}{s_1^2 + s_2^2 - s_1 s_2} \right| - \frac{3^{1/2} (s_1 + s_2) s_1 s_2}{s_1 - s_2} \\ &\left. \times \arctg \frac{3^{1/2} \alpha (s_1 - s_2)}{2(s_1^2 + s_2^2 - s_1 s_2) + \alpha(s_1 + s_2)} \right\}. \end{aligned}$$

Correspondingly, for $a > 1$ and $a > 2^{-1/3}$

$$\begin{aligned} &- \left\{ \frac{y_1^2}{(y_1 - y_2)(y_1 - y_3)} \ln \left| 1 - \frac{\alpha}{y_1} \right| \right. \\ &+ \frac{y_2^2}{(y_1 - y_2)(y_2 - y_3)} \ln \left| 1 - \frac{\alpha}{y_2} \right| \\ &\left. + \frac{y_3^2}{(y_2 - y_3)(y_3 - y_1)} \ln \left| 1 - \frac{\alpha}{y_3} \right| \right\}, \end{aligned}$$

and for $a = 1$ and $a = 2^{-1/3}$ both integrals are equal to $\frac{1}{3} (\frac{1}{3} \ln 2 - 1/2)$. Here $s_{1,2} = [2 - \alpha^3 \pm 2(1 - \alpha^3)^{1/2}]^{1/3}$, $y_1 = 2\alpha \cos \theta/3$, $y_{2,3} = -2\alpha \cos \theta \pm \pi/3$, $\theta = \arccos 2 - \alpha^3/\alpha^3$ for the first integral and $s_{1,2} = [1 - \alpha^3 \pm (1 - 2\alpha^3)^{1/2}]^{1/3}$, $y_1 = 2\alpha \cos \theta/3$, $y_{2,3} = -2\alpha \cos \theta \pm \pi/3$, $\theta = \arccos 1 - \alpha^3/\alpha^3$ for the second integral.

The second term on the right-hand side of the expression (22) is the sum of fan diagrams and the third term is the sum of ladders, each step of which is a sum of fans. The fan diagrams, as we know, describe the interference of the probability amplitudes corresponding to the two alternative ways a photon can go around a loop in a self-intersecting trajectory. The ladders describe the interference of the amplitudes corresponding to forward and backward passage of the same open chain of particles by the photon. Both interference processes are constructive: In the first case the change in phase of the wave function of the photon going around a loop is $\Delta\varphi = \oint \mathbf{k} \cdot d\vec{l} = 0$ (Ref. 12) and in the second case the phases of both virtual photons are identical. The anomalous per-particle scattering of light of both polarizations, which is associated with the interference, under conditions of close packing is shown in Fig. 5, where we resolved the scattering phase function into a sum of three components: 1) Rayleigh scattering by an isolated particle, 2) contribution of fans, and 3) contribution of ladders whose steps are sums of fans. It is clear that the enhanced light scattering into the back hemisphere for the packing factors under consideration is determined by the fans (analysis of the expression (22) shows that as $f \rightarrow 0$ both ladders and fans make the same contribution to the scattering phase function).

It is now clear that the physical reason for photon trapping in the system (see the preceding section) is precisely the anomalous scattering into the back hemisphere, owing to the interference phenomena associated with the loops in the photon trajectories. This anomalous scattering stimulates the formation of new loops in the trajectories, and so on. A

feedback mechanism arises in the system, and this is what leads to the autolocalization of the excitation and the transformation of the excitation into a standing electromagnetic wave.

The phase function for scattering strictly backward merits a separate analysis. The slit and cog, which are present in Fig. 5 and which are characteristic for the scattering phase function for *p*- and *s*-polarized light, respectively, have a simple explanation. Figures 6 and 7 each show two loops of the photon trajectory, the first of which is characteristic for scattering strictly backward and the second is characteristic for scattering of a photon into the back hemisphere excluding the strictly backward direction.

In the case of the scattering of *p*-polarized light with a dumbbell-shaped Rayleigh scattering phase function by an isolated particle, in the first case partial loss of radiation on the last particle of the loop occurs, while in the second case there are no such losses. This is the reason for the slit in the *p*-scattering phase function. The situation is different in the case of the scattering of *s*-polarized light with a spherically symmetric phase function, typical of an isolated particle. In the case of scattering strictly backwards along the axis of the loop (see Fig. 7) there is a narrow channel in which radiation scattered by each particle in a narrow cone near the axis of the loop accumulates. In the presence of any deviation, however small, from the direction of strictly backward scattering, the channel collapses. This is the reason for the appearance of a cog in the *s* phase function.

We now calculate the absorption cross section. Within the theory of linear electromagnetic response the cross section for the absorption of a photon of frequency ω is related with the imaginary part of the Fourier transform of the density-density correlation function of the system

$$\sigma_a = 2\pi e^2 \omega e_{k,\alpha} e_{k,\beta} \nabla_{k,\alpha} \nabla_{k,\beta} \text{Im} \int \Pi_{00}(\mathbf{r}, \mathbf{r}') \exp[-ik(\mathbf{r}-\mathbf{r}')] d\mathbf{r} d\mathbf{r}', \quad (23)$$

where

$$\Pi_{00}(\mathbf{r}, \mathbf{r}') = i \int_{-\infty}^{\infty} \langle T\rho(\mathbf{r}, \tau)\rho^*(\mathbf{r}', 0) \rangle e^{i\omega\tau} d\tau,$$

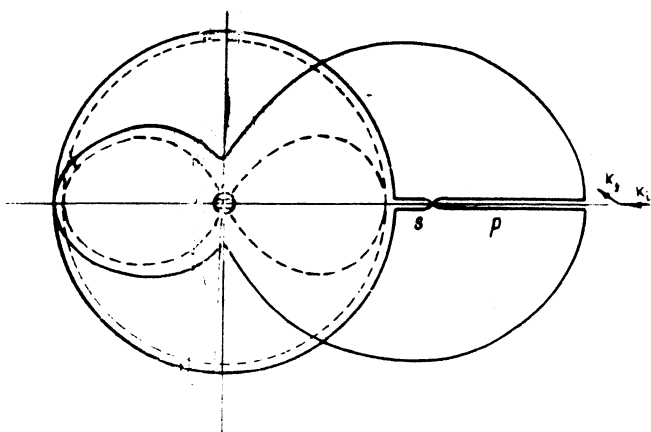


FIG. 5. Angular distribution of the intensity of *p*- and *s*-polarized light scattered by a particle in the system under conditions of strong localization ($f = 0.2$, $\omega/\omega_1 = 1.4$). The dashed curves are the Rayleigh scattering phase function and the solid curves are the contribution of the ladders (at the center) and the total phase function.

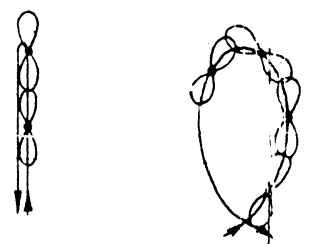


FIG. 6. Elucidation of the origin of the slit in the phase function for scattering of *p*-polarized light by a system of particles.

$\rho(\mathbf{r}, \tau)$ is the Heisenberg electron-density operator, T is the time-ordering operator, and the averaging is performed over the ground state of the electron gas of the particles of the system. It is easy to rewrite the expression (23) in terms of the photon mass operator defined in Fig. 3:

$$\begin{aligned} \sigma_a = & \frac{2\pi}{\omega} e_{k,\alpha} e_{k,\beta} \nabla_{k,\alpha} \nabla_{k,\beta} h_\gamma h_\mu \text{Im} \int \left\{ \Sigma_{\gamma\mu}(\mathbf{r}, \mathbf{r}') \right. \\ & + \int \Sigma_{\gamma\nu}(\mathbf{r}, \mathbf{r}_1) D_{\nu\mu}(\mathbf{r}_1, \mathbf{r}_2) \Sigma_{\nu\mu}(\mathbf{r}_2, \mathbf{r}') d\mathbf{r}_1 d\mathbf{r}_2 \left. \right\} \\ & \times \exp[-ik(\mathbf{r}-\mathbf{r}')] d\mathbf{r} d\mathbf{r}'. \end{aligned}$$

Simple calculations in the spirit of those recently performed give for the per-particle cross section the following expression:

$$\sigma_a = \frac{4}{3} \frac{\omega R}{c} \frac{\pi R^2}{f} \text{Im} \left\{ [\bar{\varepsilon}_t(1-g) + \bar{\varepsilon}_t g - 1] \right. \\ \left. \times \left[1-g + \frac{1-\bar{\varepsilon}_t(1-g)}{\bar{\varepsilon}_t} \right] \right\}. \quad (24)$$

Here terms $\sim (\omega R/c)^3$, associated with the retardation of electromagnetic interaction or with the escape of energy to infinity owing to the coupling of longitudinal and the transverse fields in a nonuniform system, have been dropped. The frequency dependence of the absorption cross section is presented in Fig. 4. Recall that the particles under consideration are nonabsorbing and all absorption, which is very large according to the measures adopted, is due exclusively to the localization phenomenon. One feature of the frequency dependence of the absorption cross section is its double-hump character. The point is that at the point where $d\omega/dk = 0$ and the plasmon-polariton in the system becomes a standing wave, the concept of photon motion around loops itself becomes meaningless, i.e., the physical reason for localization

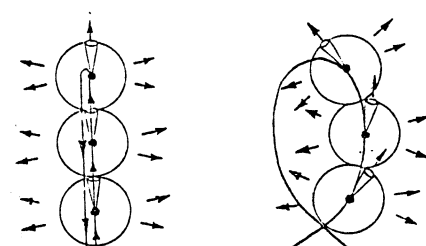


FIG. 7. Elucidation of the origin of the cog in the phase function for scattering of *s*-polarized light by a system of particles.

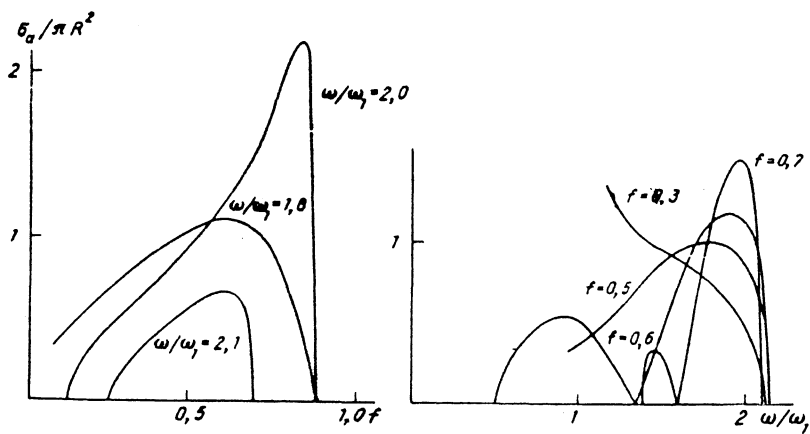


FIG. 8. Light-absorption cross section per particle in the system and associated with strong localization as functions of the packing factor and the frequency of the incident radiation.

vanishes. Correspondingly, at this location a dip appears in the absorption. The appreciably weakened character of the absorption at frequencies below the point $d\omega/dk = 0$ is associated with the indefiniteness of the plasmon-polariton in this region ($\text{Re } k \ll \text{Im } k$).

The expression (24) is noteworthy in one other respect. The absorption cross section per particle depends on the particle concentration (see Fig. 8). This is associated with the contribution of two-head, three-head, and so on diagrams in the photon mass operator. This is explained by the fact that the higher the particle concentration, the more loops form along the photon trajectory and therefore the stronger the localization. It is interesting (from the standpoint of practical applications) that the f -dependence of σ_a has a maximum, i.e., for each fixed wavelength there exists a packing for which external radiation is absorbed most effectively. The reason for the maximum is quite understandable, since for sufficiently large f localization effects vanish completely and the electrodynamic properties of the particle approach those of a continuous metal. Effects of this type should also be manifested in the breakdown of Bouguer's law, i.e., the light attenuation coefficient of a close-packed dispersed system should depend on the thickness of the sample (so-called mesoscopic effect). The physical reason for this is the same: the longer the optical path of the photon in the dispersed system, the more loops can form along the photon trajectory. Near localization thresholds the absorption cross section exhibits a characteristic nonanalytic behavior as functions of both f and ω (see Fig. 8):

$$\sigma_a \propto (f^* - f)^{\alpha_1} \text{ for } f < f^* \text{ and } \sigma_a = 0 \text{ for } f > f^*,$$

$$\sigma_a \propto (\omega^* - \omega)^{\alpha_2} \text{ for } \omega < \omega^* \text{ and } \sigma_a = 0 \text{ for } \omega > \omega^*,$$

—as expected result of the scaling approach to the problem.

5. CONCLUSION

The aim of this paper was to elucidate the mechanism of strong localization of light in a dispersed medium. We established that this phenomenon is associated with the loops that form in photon trajectories. If a photon forms a loop, then the interference of the probability amplitudes corresponding to the two possible ways of going around this loop—clockwise and counterclockwise—intensifies light scattering into the back hemisphere. This stimulates the formation of new loops in the trajectory, and so on. As a result the photon is trapped in a spatial region of characteristic size $\sim \lambda \approx l_s$,

forming a standing electromagnetic wave.

Loops are not always formed on the photon trajectory. In order for loops to form, the photon elastic scattering length l_s must be of the same order of magnitude as the photon wavelength λ . In a system of close-packed ultradispersed metallic particles, with which we are concerned, $l_s \gg \lambda$ almost always. The range of frequencies near the frequency of the dipole surface plasmon in an isolated particle, where l_s decreases in a resonance fashion, is an exception. This resonance plays the role of a primer that initiates the localization process.

Strong localization is manifested in experiment primarily as anomalous light attenuation by the system. This anomalous attenuation is associated with the accumulation of electromagnetic radiation in the form of standing waves in the system. In addition, the light attenuation coefficient of a dispersed system starts to depend on the sample size, i.e., Bouguer's law breaks down.

It is interesting that the phenomenon of strong localization of light, at first glance, already appears in the mean-field theory. Indeed, the standard mean-field theory is obtained from our calculations, if the calculations are limited to the single-site variant of the coherent-potential approximation, i.e., the multihead diagrams in the perturbation series for the photon mass operator Σ are neglected. In this case $\bar{\epsilon}_i = \bar{\epsilon}_j = \bar{\epsilon}$, and the equation for $\bar{\epsilon}$ can be easily derived from Eq. (17) and has the form

$$\frac{\bar{\epsilon} - 1}{3\bar{\epsilon}} = g \frac{\bar{\epsilon} - \bar{\epsilon}}{\bar{\epsilon} + 2\bar{\epsilon}}. \quad (25)$$

This equation is reminiscent of Bargmann's well-known equation for the effective dielectric constant of a dispersed medium.¹⁰ if we set $\bar{\epsilon} = 1 - \omega_0^2/\omega^2$, then in spite of the fact that a metallic particle in this case is absolutely nonabsorbing, it follows from Eq. (25) that in a definite region of f and ω the dielectric constant $\bar{\epsilon}$ will be complex, i.e., there arises some mysterious absorption or attenuation of radiation in the system. The reason for this, however, is quite prosaic and is totally unrelated to strong localization. Thus if we write the average amplitude of forward scattering of a photon as

$$\begin{aligned} \langle \mathcal{T}(0) \rangle = & e_{i\alpha} \int \exp(-ik_i \mathbf{r}) t_{\alpha\gamma}(\mathbf{r}, \mathbf{r}') e_{\gamma} \exp(ik_i \mathbf{r}') d\mathbf{r} d\mathbf{r}' \\ & + e_{i\alpha} \int \exp(-ik_i \mathbf{r}) t_{\alpha\beta}(\mathbf{r}, \mathbf{r}_1) D_{\beta\gamma}(\mathbf{r}_1, \mathbf{r}_2) t_{\gamma\nu}(\mathbf{r}_2, \mathbf{r}') \\ & \times \exp(ik_i \mathbf{r}') e_{\nu} d\mathbf{r} d\mathbf{r}_1 d\mathbf{r}_2 d\mathbf{r}', \end{aligned}$$

then after simple calculations we will see that $\langle \mathcal{T}(0) \rangle = 0$. Therefore the optical theorem completely forbids any attenuation of light in the system and the nonzero absorption is related exclusively with the deficiencies of this approximation. As we can see, different considerations must be invoked in order to explain the true reason for the absorption. We wish to say a few words about the validity of the approximations which we employed. We neglected correlations in the spatial arrangement of the particles. Taking such correlations into account does not lead to qualitatively new phenomena pertaining to localization. Systems with long-range correlations, for example, fractal clusters, are an exception.

- ² Yu. N. Barabanenko, Izv. Vysh. Uchebn. Zaved., Radiofiz. **16**, 88 (1973).
- ³ A. G. Vinogradov, Yu. A. Kravtsov, and V. I. Tatarskii, Izv. Vysh. Uchebn. Zaved., Radiofiz. **16**, 1064 (1973).
- ⁴ P. P. Gor'kov, A. N. Larkin, and D. E. Khmel'nitskii, Pis'ma Zh. Eksp. Teor. Fiz. **30**, 248 (1979) [JETP Lett. **30**, 228 (1979)].
- ⁵ A. A. Golubentsev, Zh. Eksp. Teor. Fiz. **86**, 47 (1984) [Sov. Phys. JETP **59**(1), 26 (1984)].
- ⁶ E. E. Gorodnichev, S. A. Dudarev, D. B. Rogozkin, and M. I. Ryzanov, Zh. Eksp. Teor. Fiz. **96**, 1801 (1989) [Sov. Phys. JETP **69**(5), 1017 (1989)].
- ⁷ M. Kaveh, Phil. Mag. **56**, 693 (1987).
- ⁸ S. John, Phys. Rev. Lett. **53**, 2169 (1984).
- ⁹ K. Arya, Z. B. Su, and J. L. Birman, Phys. Rev. Lett. **57**, 2725 (1986).
- ¹⁰ C. F. Bohren and D. R. Huffman, *Absorption and Scattering of Light by Small Particles*, Wiley, N. Y., 1983.
- ¹¹ L. D. Landau and E. M. Lifshitz, *Electrodynamics of Continuous Media*, Pergamon Press, N. Y.
- ¹² A. A. Abrikosov, *Principles of the Theory of Metals*, Nauka, Moscow, 1987.

Translated by M. E. Alferieff

¹ P. Sheng, *Scattering and Localization of Classical Waves in Random Media*, Singapore, 1990.